

# The World Wide Lightning Location Network and Convective Activity in Tropical Cyclones

SERGIO F. ABARCA AND KRISTEN L. CORBOSIERO

*Department of Atmospheric and Oceanic Sciences, University of California, Los Angeles, Los Angeles, California*

DAVID VOLLARO

*Department of Atmospheric and Environmental Sciences, University at Albany, State University of New York, Albany, New York*

(Manuscript received 11 February 2010, in final form 19 August 2010)

## ABSTRACT

Lightning flash density in tropical cyclones (TCs) is investigated to identify whether lightning flashes provide information on TC intensity and/or intensity change, to provide further insight into TC asymmetric convective structure induced by vertical shear and storm motion, and to assess how well the World Wide Lightning Location Network (WWLLN) is suited for the observation of TCs. The 24 Atlantic basin TCs that came within 400 km of the United States from 2004 to 2007 are studied. The National Lightning Detection Network is used to analyze flash density as a function of peak current and to evaluate the WWLLN. Flash density is shown to be smaller for hurricanes than for tropical depressions and storms, with this reduction being gradually more pronounced as flash peak current increases. The results suggest that flash density in the inner core is a parameter with potential for distinguishing intensifying versus nonintensifying TCs, particularly in the weaker storm stages where flash densities are largest.

Vertical wind shear produces a strong downshear left (right) asymmetry in the inner core (outer rainbands), whereas motion asymmetries are less clear. The unprecedented azimuthal resolution used in this study suggests that as shear strengthens, the azimuthal region of convection in the inner core is sharpened from a width of  $\sim 130^\circ$  to a width of  $\sim 60^\circ$ . The radial distribution of flash density is shown to exhibit a relatively narrow region of little activity (between 60 and 120 km from the eye), with increased activity in both regions closer to, and more distant from, the center (i.e., the eyewall and outer rainbands, respectively). Finally, it is shown that the WWLLN captures the convective activity in Atlantic basin TCs remarkably well, despite its low detection efficiency.

## 1. Introduction

Lightning locations have been shown to provide valuable information in the study of tropical cyclones (TCs). The most relevant to this study are the findings on asymmetries in convection associated with vertical wind shear and storm motion by Corbosiero and Molinari (2002, 2003, hereafter CM02 and CM03, respectively). CM02 found a strong relationship between the azimuthal distribution of flashes and the direction of vertical wind shear; CM03 assessed the effects of storm motion on the distribution of convection and their relative importance

compared to those of shear. The results of these two studies were consistent with findings based on different proxies for convection (e.g., vertical motion, radar reflectivity, and rainfall), but it was only through lightning that it was clearly shown how the effects of shear dominate over those of motion.

The relationships among flash density, TC intensity, and intensity change have also been explored. Using the Optical Transient Detector (OTD; Boccippio et al. 2000), a space-borne lightning sensor aboard the *Microlab-1* (renamed *OV-1*) satellite, Cecil and Zipser (1999) analyzed two hurricane seasons in the Atlantic and eastern and western Pacific Oceans and found an increased likelihood of inner core lightning in weak tropical storms and strong hurricanes/typhoons. They found no clear relationship between lightning observations and TC intensification, but the detection efficiency (approximately 55%) and

---

*Corresponding author address:* Sergio F. Abarca, Department of Atmospheric and Oceanic Sciences, University of California, Los Angeles, 405 Hilgard Ave., Los Angeles, CA 90095.  
E-mail: abarcas@atmos.ucla.edu

short view time of the OTD (less than 5 min) may have obscured their results. Molinari et al. (1999) studied lightning in nine Atlantic hurricanes using data from the National Lightning Detection Network (NLDN) and found no clear relationship between average lightning frequency and storm intensity; however, their study was limited to storms within 400 km of the U.S. coastline and their intensification sample was rather limited. More recently, Leary and Ritchie (2009) used data from the Long-Range Lightning Detection Network (LLDN; Cramer and Cummins 1999; Cummins et al. 1999; Demetriades and Holle 2005, 2006; Pessi et al. 2009) to successfully distinguish developing from nondeveloping tropical cloud clusters during the 2006 eastern Pacific TC season. Squires and Businger (2008), also using data from the LLDN, found eyewall lightning outbreaks during the periods of rapid intensification in Hurricanes Rita and Katrina (2005). These findings were consistent with the large number of flashes (as high as  $600 \text{ h}^{-1}$ ) reported by Shao et al. (2005) in Rita and Katrina as detected by the Los Alamos National Laboratory's Sferic Array.

The World Wide Lightning Location Network (WWLLN) has also been used to study TC intensification. DeMaria and DeMaria (2009) studied flash density and its relationship to intensity change for Atlantic basin TCs between 2005 and 2007. Their results suggest some potential for using flash density to predict rapid intensification. Price et al. (2009) found that 56 of 58 category 4 and 5 hurricanes/typhoons they analyzed showed a significant correlation (mean of 0.82) between maximum sustained winds and lightning frequency, with increased lightning activity approximately one day prior to peak intensity. Thomas et al. (2010) found episodic inner core lightning outbreaks prior to and during most changes in storm intensity (strengthening and weakening) of Hurricanes Rita, Katrina, and Emily (2005). They also found an increase in the relative number of positive cloud-to-ground (CG) flashes in the inner core prior to and during periods of storm weakening.

A number of authors have also described the radial structure of flash density in TCs (Molinari et al. 1994, 1999; Cecil et al. 2002; Cecil and Zipser 2002; Squires and Businger 2008; Yokoyama and Takayabu 2008) and found two maxima of flash density, one within 100 km of the center and a second one farther out in the rainbands; however, the magnitude and the relative strengths of these maxima have varied significantly among the studies. Molinari et al. (1994), using the NLDN in Hurricane Andrew (1992), found a weak maximum in the eyewall, a region of near-zero flash density 40–100 km from the center, and a steady increase to a larger maximum in the outer bands. Molinari et al. (1999) also found the greatest flash density in the rainband region with a smaller, relative

maximum in the inner core. Yokoyama and Takayabu (2008), however, using six years of Tropical Rainfall Measuring Mission (TRMM; Kummerow et al. 1998) data, found a lightning maximum in the inner core, with larger flash density in stronger TCs, in agreement with the results of Squires and Businger (2008).

Despite efforts to investigate the various aspects of lightning in TCs noted above, lightning data available for TC research have been strongly spatiotemporally limited. The characteristics of these limitations depend on the technology used to detect the flashes. Satellite-borne lightning measurements (Cecil and Zipser 1999; Cecil et al. 2002) are confined to a few minutes of data, at most twice a day. Aircraft data (Black and Hallett 1999) are even more spatiotemporally restricted to individual flight legs. Land-based networks, with continuous coverage, have been the most convenient platform to observe lightning in TCs, but their domain of observation is confined to the continent and adjacent waters with poor coverage over the open ocean. In TC research, the NLDN has been successfully used (Molinari et al. 1994, 1999; Samsury and Orville 1994; CM02; CM03), leading to the results discussed above. This land-based network has the advantages of very high detection efficiency (DE) and location accuracy (LA), but its coverage is limited to continental North America and adjacent oceans, with its DE and LA decreasing quickly with the distance from the shore (Cummins and Murphy 2009).

Given the spatial constraints of the NLDN, the Vaisala Thunderstorm Group developed the LLDN, a network that uses the sensors of the NLDN and those of the Canadian Lightning Detection Network in the very low frequency (VLF) band to locate lightning with a range of detection an order of magnitude larger than that of the NLDN. The LLDN has been used in TC research by Squires and Businger (2008) in an attempt to overcome the spatial limitations of the NLDN, but the LLDN is still limited to the adjacent oceans of continental North America. In addition to the LLDN, Vaisala has recently developed a global lightning network, the Global Lightning Dataset (GLD360) (<http://www.vaisala.com/weather/products/gld360.html>; Demetriades et al. 2010), but information about its DE and LA is limited at this time.

The WWLLN has global coverage and can be used to overcome the spatiotemporal limitations that TC research examining lightning has had. The WWLLN is relatively new, is in the process of development, and its DE is still low; however, a statistical proportionality between flashes located by the WWLLN and by networks with higher DE has been suggested (Jacobson et al. 2006; Abarca et al. 2010). If the WWLLN can be used to overcome the spatiotemporal limitations that lightning research in TCs has had, it is worth analyzing whether flash density carries information regarding storm intensity and intensification,

and how well the conclusions obtained with higher DE networks can be reproduced by the WWLLN. This article addresses these two questions and has the overarching goal of showing the utility of the WWLLN data in TC research.

## 2. Data sources

### a. Lightning data

The WWLLN provides lightning locations by detecting sferics: lightning-driven signals in the VLF band (3–30 kHz). The electromagnetic energy within the VLF band propagates with low attenuation in the earth–ionosphere waveguide and its signal can be detected thousands of kilometers from the source (Crombie 1964). The network detects CG and intracloud (IC) flashes with the same efficiency as long as they have the same current magnitude and channel length (Lay et al. 2004; Rodger et al. 2005, 2006; Jacobson et al. 2006); however, CG DE is about twice the IC DE (Abarca et al. 2010) because CG flashes tend to have higher peak currents. The stable propagation and low attenuation of VLF waves in the earth–ionosphere waveguide allows a spacing of the receiver sites of thousands of kilometers, but the ionospheric interaction spectrally distorts the received waveform so that it is not straightforward to infer the vertical current magnitude or polarity. Following the advice of the WWLLN developers, only those lightning locations that triggered at least five sensors and that had residuals  $\leq 30 \mu\text{s}$  are regarded as good locations and are included in this analysis. The processing algorithm used here is the latest released, which has been estimated to generate 63% more lightning locations than previous algorithms (Rodger et al. 2009).

The WWLLN's DE and LA have been estimated by comparison with regional lightning detection networks and with idealized models. The first WWLLN evaluation published (Lay et al. 2004) was performed during March 2003, when only 11 WWLLN sensors were active, mostly in Oceania and Southeast Asia. The evaluation was performed in a region of Brazil against the Brazilian Integrated Network (Pinto and Pinto 2003) and resulted in an estimated DE of about 0.3% and an LA of  $20.25 \pm 13.5$  km. Figure 1a shows the distribution of the 19 WWLLN sensors (circles) operational during the summer of 2004 when three other WWLLN evaluations were performed. The first of these three studies (Rodger et al. 2005) focused on a region in Australia, where the WWLLN DE was estimated to be  $\sim 26\%$  for CG and  $\sim 10\%$  for IC flashes. The overall LA was estimated to range over 1.9–19 km with a median of 2.9 km. The second evaluation (Rodger et al. 2006) took place in New Zealand and estimated an overall DE of 5.4% with a higher DE (9%–10%)

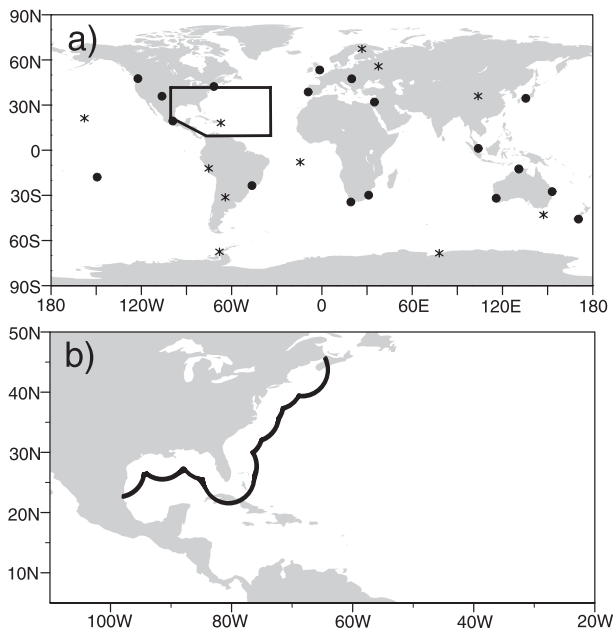


FIG. 1. (a) WWLLN network configuration and domain of study (polygon in the Atlantic). Circles indicate the locations of the 19 active stations during the summer of 2004, and asterisks indicate the locations of the 11 stations installed between that time and the end of 2007. (b) Enlarged domain of study indicating the region up to about 400 km away from the U.S. shore (black curved line) where the WWLLN was compared with the NLDN.

for those discharges larger than  $\pm 50$  kA. The third evaluation was carried out over Florida (Jacobson et al. 2006), where the DE was considerably lower: 1% overall and 4% for those strokes with currents larger than  $\pm 30$  kA. The LA was estimated to be around 15 km in this region with very few sensors in 2004.

The most comprehensive evaluation of the WWLLN was conducted by Abarca et al. (2010). They realized a continental-scale, multiyear (2006–09) study evaluating the WWLLN using the NLDN as ground truth. They found a consistent time improvement of the CG DE from 3.88% (April 2006–March 2007) to 10.30% (April 2008–March 2009). Abarca et al. (2010) also found average LAs in the meridional and zonal directions of 4.03 and 4.98 km, respectively.

The NLDN was originally developed at the University at Albany and is currently operated by the Vaisala Thunderstorm Unit (Cummins and Murphy 2009). The NLDN detects lightning using both time-of-arrival and direction information via “Improved Accuracy through Combined Technology” Enhanced Sensitivity and Performance sensors. Since April 2006, all events with peak currents between 0 and 15 kA and all positive (negative) events with a peak-to-zero (PTZ) time  $\leq 15 \mu\text{s}$  ( $\leq 12 \mu\text{s}$ ) are considered cloud discharges and are eliminated from

TABLE 1. List of storms and the hours they were within the evaluation domain. The last four columns show the number of ITPs in which each of the networks reported lightning in the inner core (0–100 km from the center) and the outer bands (100–300 km from the center).

Year	Storm	Times				Periods with flashes			
		Begin		End		NLDN		WWLLN	
		Hour (UTC)	Date	Hour (UTC)	Date	Inner core	Outer bands	Inner core	Outer bands
2004	Bonnie	1200	11 Aug	1800	13 Aug	7	7	7	7
	Charley	1200	13 Aug	1800	14 Aug	4	4	4	4
	Frances	0000	04 Sep	1800	08 Sep	3	18	1	16
	Gaston	1200	27 Aug	0000	01 Sep	14	17	8	17
	Hermine	1200	30 Aug	0600	31 Aug	2	2	2	2
	Ivan	1200	15 Sep	0600	24 Sep	4	11	2	9
	Jeanne	1200	25 Sep	1800	28 Sep	2	10	0	7
	Matthew	1200	08 Oct	1800	10 Oct	8	8	6	8
2005	Arlene	0000	11 Jun	0600	13 Jun	3	8	2	6
	Cindy	1200	05 Jul	0600	07 Jul	6	6	1	6
	Dennis	0000	09 Jul	0600	13 Jul	7	12	4	6
	Emily	1200	19 Jul	1200	21 Jul	5	5	3	5
	Katrina	0000	25 Aug	1800	30 Aug	19	20	18	20
	Ophelia	0600	06 Sep	1800	17 Sep	26	43	24	41
	Rita	0000	23 Sep	0000	26 Sep	6	9	3	9
	Tammy	0600	05 Oct	1800	06 Oct	4	5	3	4
	Wilma	0000	24 Oct	0000	25 Oct	3	3	2	3
2006	Alberto	0600	12 Jun	0600	14 Jun	4	7	4	7
	Beryl	1200	18 Jul	1200	21 Jul	5	11	5	10
	Ernesto	1200	24 Aug	1200	01 Sep	10	11	9	10
2007	Barry	0600	02 Jun	1800	02 Jun	1	1	1	1
	Erin	1200	15 Aug	0600	17 Aug	6	6	6	6
	Gabrielle	0000	09 Sep	0000	11 Sep	4	7	5	7
	Humberto	1200	12 Sep	0000	14 Sep	4	5	4	5
Total					157	236	124	216	

the database (Fleener et al. 2009). Before April 2006, only those flashes that had a PTZ time  $\leq 10 \mu\text{s}$  were classified as cloud pulses (regardless of their peak current). NLDN evaluation experiments (carried out using an optical sensor and a broadband electric field antenna) during 2003 and 2004 show a NLDN flash DE of 93% in Arizona and 92% in Texas and Oklahoma (Biagi et al. 2007); these experiments also show LAs with a median of 0.424 km in Arizona and 0.279 km in Texas and Oklahoma.

### b. Best-track and wind shear data

The National Hurricane Center (NHC)–Tropical Prediction Center (TPC) best-track dataset was used to obtain tropical cyclone latitude, longitude, and intensity. These data have a temporal resolution of 6 h and were linearly interpolated to hourly values to estimate the position of lightning flashes with respect to the storm center. The best-track data were also used to estimate a motion vector and determine whether a storm was intensifying.

The European Centre for Medium-Range Weather Forecasts (ECMWF) gridded analyses, with horizontal resolution of  $1.125^\circ$  and 13 vertical pressure levels, were used to compute environmental vertical wind shear between 850 and 200 hPa every 6 h following Molinari and

Vollaro (1989). At each level, the cylindrical area weighted averages of the mean wind's Cartesian components were computed over a radius of 500 km so that the symmetric vortex was removed and the resulting winds were a measure of the cross-storm flow. Further discussion of the characteristics and reliability of these calculations can be found in CM02.

## 3. Data sample and methodology

### a. Domain and data sample

The 24 Atlantic basin TCs that occurred between 11 August 2004 and 14 September 2007 and came within 400 km of the U.S. shore are examined in this study. As in CM02 and CM03, the results were not grouped by storm; instead the data were grouped in sets of 6-h periods herein called individual time periods (ITPs). For analysis, ITPs were grouped in two domains. The first of these domains, herein called the evaluation domain, was used to assess the performance of the WWLLN compared with the NLDN and consists of those ITPs in which the storm centers were within 400 km of at least one NLDN sensor where the NLDN is most reliable (Table 1). Figure 1b shows the Atlantic basin with a scalloped line of about

TABLE 2. List of storms and the hours they were within the ocean domain. The last four columns show the number of ITPs in which the WWLLN reported lightning in the inner core (0–100 km from the center) and the outer bands (100–300 km from the center). The “Rotation” data refer to 6-h ITPs centered on 0000, 0600, 1200, and 1800 UTC (e.g., 2100–0300 UTC is centered on 0000 UTC) used to rotate flashes with respect to shear and motion vectors. The “Intensification” data refer to ITPs spanning the 6-h periods between available best-track times (i.e., 0000–0600 UTC), used to identify whether the storm was intensifying.

Year	Storm	Times				Periods with flashes			
		Begin		End		Rotation		Intensification	
		Hour (UTC)	Date	Hour (UTC)	Date	Inner core	Outer bands	Inner core	Outer bands
2004	Bonnie	1200	08 Aug	1200	11 Aug	2	2	2	1
	Charley	1200	09 Aug	1200	13 Aug	6	7	6	6
	Frances	0000	25 Aug	0000	04 Sep	20	39	21	38
	Hermine	1800	27 Aug	1200	30 Aug	9	10	8	9
	Ivan	1800	02 Sep	1200	15 Sep	38	46	37	44
	Jeanne	1800	13 Sep	1200	25 Sep	29	45	28	43
2005	Arlene	1800	08 Jun	0000	11 Jun	4	8	2	6
	Cindy	1800	03 Jul	1200	05 Jul	1	6	1	5
	Dennis	1800	04 Jul	0000	09 Jul	11	16	10	15
	Emily	0000	11 Jul	1200	19 Jul	29	33	25	31
	Katrina	1800	23 Aug	0000	25 Aug	4	4	3	3
	Rita	0000	18 Sep	0000	23 Sep	19	19	18	17
2006	Wilma	1800	15 Oct	0000	24 Oct	18	31	17	31
	Alberto	0600	10 Jun	0600	12 Jun	2	7	3	7
	Ernesto	1800	24 Aug	1200	29 Aug	15	15	14	15
2007	Barry	1200	01 Jun	0600	02 Jun	2	2	1	2
Total						209	290	196	273

400 km from the U.S. shore, separating the evaluation domain from the other domain of this study, herein called the open ocean domain (see Fig. 1a and Table 2). The open ocean domain is made up of those ITPs that occurred before the storms reached the evaluation domain and was used to compare the lightning characteristics of intensifying versus nonintensifying ITPs. The azimuthal and radial structures of flash occurrence were analyzed separately in both domains. For the ITPs with flashes, all discharges within 300 km of the hourly interpolated centers were included. With each of these individual time periods are associated a unique shear vector, motion vector, and lightning distribution. To evaluate the effect of the shear and motion on the azimuthal distribution of lightning, the flashes in each ITP were separately rotated around the storm center so that the vector under consideration was pointing due north.

With the idea that only those ITPs with a relatively large number of flashes can meaningfully indicate where the maximum of lightning activity is occurring, CM02 imposed minimum flash criteria. The effects of imposing criteria such as those used in CM02 on the data of this study were thoroughly examined and proven not to affect the conclusions that could be drawn and that such an imposition strongly limited the number of ITPs. In view of these results, this study does not include any minimum flash criteria and all ITPs are considered as valid data points as long as they have at least one flash.

*b. Azimuthal distribution*

Any straight count of flash occurrence would be skewed by ITPs that contain large amounts of lightning since the number of flashes in each ITP varied from one to thousands. In the NLDN (WWLLN), the ITP with the largest amount of flashes accounts for 3% (5%) of the total amount of flashes examined. To avoid having a few extreme events dominate the azimuthal distribution of flashes and to allow each ITP to have equal weight, CM02 and CM03 analyzed not only the flash count itself but also the number of ITPs with the maximum number of flashes in each shear or motion-rotated quadrant or octant. In this study, for each ITP, the number of flashes is counted in 20 sectors, each of them spanning an azimuth of 18°. This allows analysis, with unprecedented resolution, of the azimuthal distribution of flashes. The sum in each sector is normalized by the largest sum in the 20 sectors so that each sector has a value from 0 to 1. Next, all sector values from each ITP are summed. To analyze the results, the normalized sums are plotted as the vertices of 20-sided polygons (hereafter icosagons) around the storm center. Each vertex is plotted at a radius proportional to the normalized sum in the direction of the center of the sector. The vertices are connected to form icosagons and their shapes are studied.

The azimuthal asymmetries are studied in two storm regions: the inner core (0–100 km) and the outer bands

(100–300 km), following CM02 and CM03. This choice follows from the findings of Molinari et al. (1994, 1999) and Squires and Businger (2008), who distinguished a clear minimum in the radial distribution of flash density between 60 and 140 km from the center of TCs.

#### 4. WWLLN versus NLDN storm detection efficiency

As a way to test the WWLLN's ability to capture the electrical discharge activity occurring in TCs, we apply the method proposed by Jacobson et al. (2006) in the evaluation domain. This method, also used by Abarca et al. (2010), is designed to evaluate the statistical proportionality of the discharge detection between the WWLLN and the NLDN. Some proportionality is expected, but since the two networks aim at different aspects of lightning activity (the NLDN focuses only on CG flashes, whereas the WWLLN has a tendency to detect stronger flashes regardless of their type), it is not expected that the networks are fully proportional.

Each ITP's flashes are integrated into a matrix with a pixel size of  $0.2^\circ$  latitude  $\times$   $0.2^\circ$  longitude. This pixel size is less than 4% of the considered diameter of the storm (600 km). As Jacobson et al. (2006) proposed, we count the number of flashes located in each pixel by each network and denominate the matrices composed of these sums as  $N_W(j, k, m)$  and  $N_N(j, k, m)$  for the WWLLN and NLDN, respectively. The following quantities are also computed:

$$A_{Wm} = \sum_j \sum_k N_W^2(j, k, m), \quad (1)$$

$$A_{Nm} = \sum_j \sum_k N_N^2(j, k, m), \quad \text{and} \quad (2)$$

$$C_{NWm} = \sum_j \sum_k N_N(j, k, m) N_W(j, k, m), \quad (3)$$

where  $A_{Wm}$  and  $A_{Nm}$  are the sums of all the bins in the domain for time  $m$  for the WWLLN and the NLDN, respectively, where each time  $m$  represents one ITP;  $C_{NWm}$  is the covariance of the networks. The normalized spatial correlation (SC) between the NLDN and WWLLN is the ratio of  $C_{NWm}$  to the geometric mean of  $A_{Nm}$  and  $A_{Wm}$ .

The SC is shown in Fig. 2 versus the geometric mean of the WWLLN and NLDN autocovariances. It shows that the SC can take any value between 0 and 1 and that there is a tendency toward higher SC as the geometric mean of the WWLLN and NLDN grows; that is, as the number of flashes detected by the networks increases, so does the spatial correlation parameter SC. The median value of the

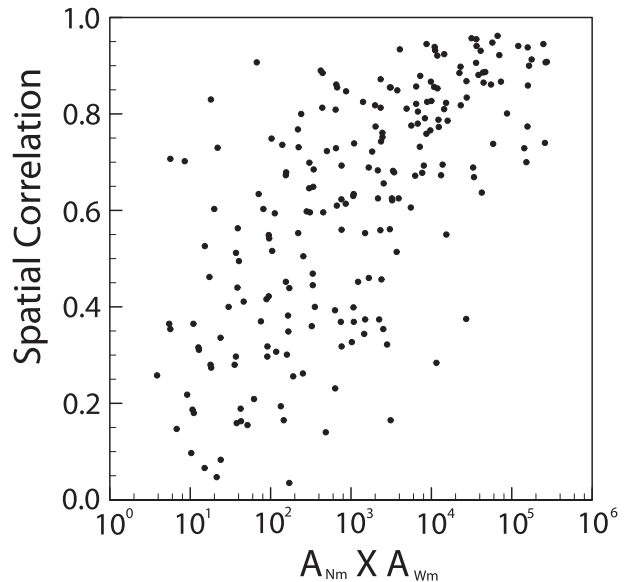


FIG. 2. Scatterplot of spatial correlation (defined in the text) as a function of the geometric mean of the WWLLN and NLDN autocovariances.

SC obtained here is 0.67, which is within the range of values obtained by Abarca et al. (2010) but larger than the value of 0.61 found by Jacobson et al. (2006). One reason for this might be that the Jacobson et al. (2006) study took place in the summer of 2004 when only 19 sensors made up the WWLLN (and only 4 in North America; see Fig. 1a). In 2005, 2006, and 2007, the number of WWLLN sensors consistently increased to 23, 28, and 30, respectively. About 33% of the ITPs in this study were collected during 2004, with most (47%) of the ITPs in 2005 and only 12% and 8% in 2006 and 2007, respectively.

The strong spatial correlation found in the sample of this study suggests that, despite the fact that the two networks do not target exactly the same discharges, the lightning activity is well captured by the WWLLN, in agreement with previous studies (Jacobson et al. 2006; Abarca et al. 2010).

#### 5. Flash density, storm intensity, and intensification

With the confidence of the statistical proportionality analysis of section 4, a quantification of the number of flashes in the open ocean domain was performed. Figure 3 shows the average flash density for intensifying and nonintensifying (defined as the 6-h intensity change between best-track data points) ITPs in the inner core and outer band regions. It shows that for all storm categories studied, the average number of flashes in the inner core (Fig. 3a) is larger in intensifying ITPs. Intensifying tropical storms and tropical depressions (category TDTS) have on

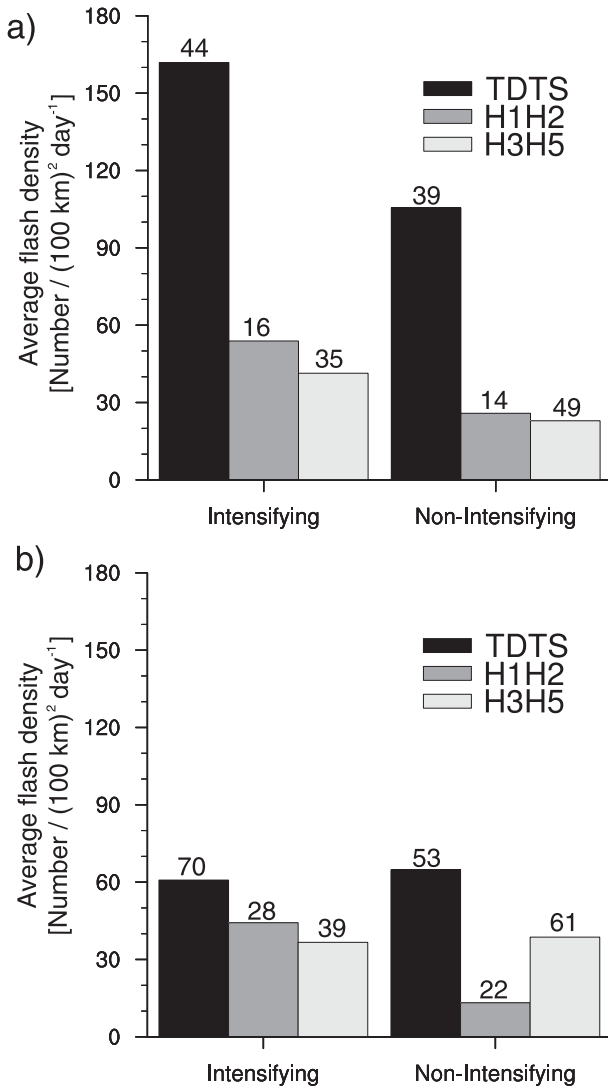


FIG. 3. WWLLN average flash density for intensifying and non-intensifying ITPs in the open ocean domain for the (a) inner core and (b) outer bands. Storm intensity is separated in three categories: tropical depressions and tropical storms (TDTs), category 1 and 2 hurricanes (H1H2), and category 3, 4, and 5 hurricanes (H3H5). The number on top of each bar indicates the number of ITPs used for the average.

average about 1.5 times more flashes than their nonintensifying counterparts. Intensifying category 1 and 2 hurricanes (category H1H2; 33–49 m s<sup>-1</sup>) and category 3, 4, and 5 hurricanes (category H3H5; >50 m s<sup>-1</sup>) have approximately 2 times more flashes than nonintensifying cases. For the outer bands, where the average flash density is substantially smaller (Fig. 3b), no significant differences between intensifying and nonintensifying ITPs are evident except for intensifying H1H2 storms that have more than 3 times the number of flashes of nonintensifying H1H2 TCs. Figure 3 also shows that, on average, weaker storms have a

substantially larger amount of flashes in the inner core than in the outer bands; however, the straight averaging of flash counts may not be the best way to compare inner core and outer bands flash densities, as is further explored in section 7.

Larger average flash density in the inner core of intensifying storms, particularly in intensifying weak storms, might be the result of a more efficient charging mechanism in TCs undergoing intensification. Black and Hallett (1999) summarize two decades of TC microphysical research and explain the electrification of the hurricane in terms of the graupel–ice mechanism (Rakov and Uman 2003). In the TC’s inner core, coalescence is very effective and many drops rain out from updrafts before they reach the mixed phase region. This region is usually relatively shallow, limited to temperatures above about -5°C (the characteristic TC updraft is relatively weak, yielding relatively small amounts of supercooled water). Intensifying TCs, exhibiting stronger vertical wind speeds (>20 m s<sup>-1</sup>; Black et al. 1994), may have higher mixed phase regions, larger concentrations of supercooled water, a more efficient charging mechanism, and higher flash density. This mechanism might be less effective as the storm organizes (H1H2 and stronger), since a larger availability of preexisting ice in the inner core (which efficiently nucleates supercooled water) may limit the charging mechanism and therefore flash density.

### 6. Azimuthal asymmetries

The azimuthal distribution of lightning in TCs induced by shear and motion is explored in both study domains. To facilitate the interpretation of the results, Fig. 4 presents, for each domain, the distributions of ITPs with flashes as a function of shear and motion vector magnitude versus TC intensity. Overall, as storm intensity increases, there tend to be fewer ITPs with high shear and slow motion, particularly in the evaluation domain, where there are no category 4 or 5 ITPs with strong shear or slow motion. Although the open ocean domain has a better representation of different storm intensities at the different shear and motion magnitudes considered, there still are no cases of intense hurricanes (category 3 and stronger) with strong shear, or category 5 hurricanes with slow motion. Figure 4 shows that the distribution of ITPs with respect to the magnitudes of shear and motion tends to be the same in both the NLDN (top row) and the WWLLN (middle row) in the evaluation domain.

#### a. Shear asymmetries in the inner core

Figures 5a–f show inner core lightning locations for all NLDN and WWLLN ITPs after the flashes were rotated so that the shear vector for each ITP points due north.

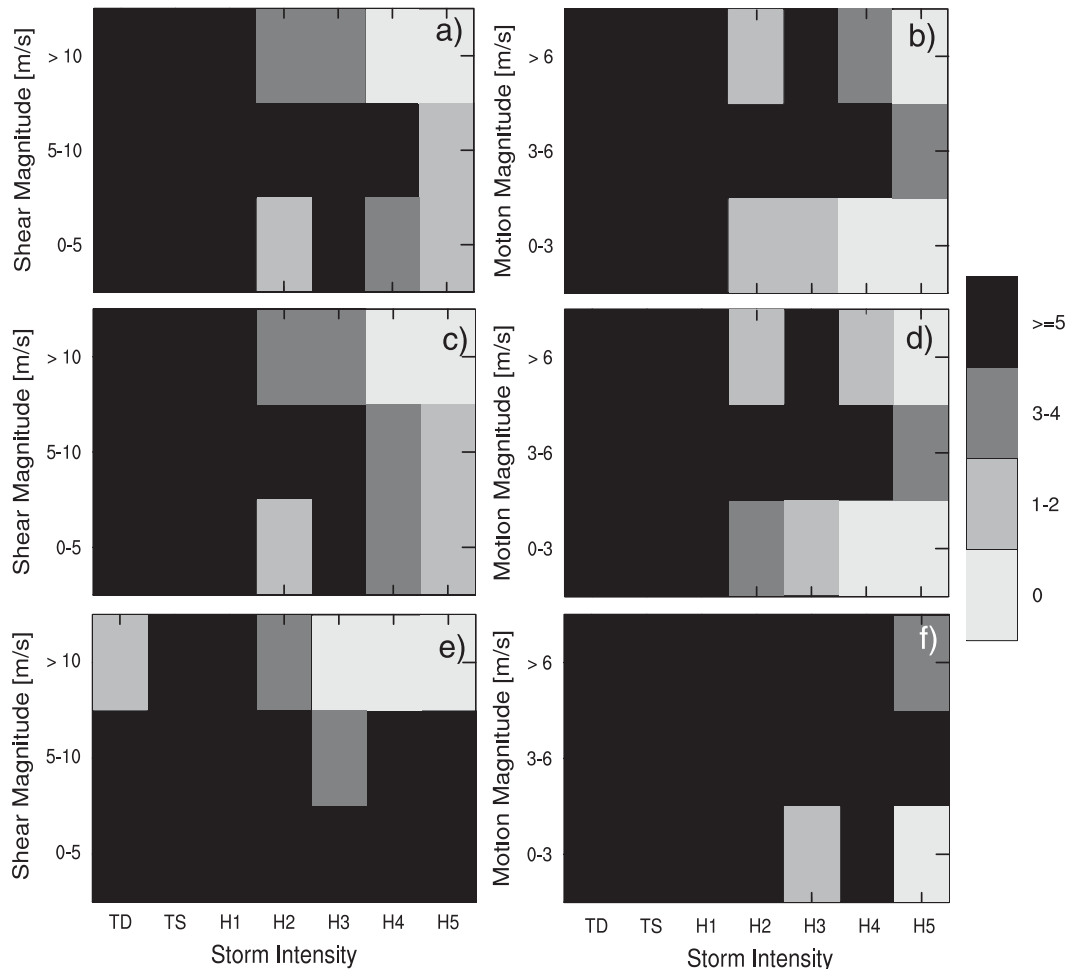


FIG. 4. Individual time period availability as a function of (left) shear and (right) motion magnitude. (top),(middle) Evaluation domain (with the NLDN in the top row and the WWLLN in the middle row). (bottom) Open ocean domain (WWLLN only).

Despite the large differences in the number of flashes between the networks, it can be seen that they roughly agree on the structure of the lightning distribution, both azimuthally and radially. The areas around the storm center with clusters of lightning in the NLDN are captured, although with reduced detail, by the WWLLN.

Although location plots of individual flashes are useful for an initial visual comparison, they can be misleading since ITPs with large numbers of flashes may be contributing a large number of flashes in regions other than that of maximum activity, and these flashes might obscure the signal of other ITPs with fewer flashes. As an example of this phenomenon, the strong shear flash plots (Figs. 5c,f) will erroneously lead to the conclusion that the maximum in flash occurrence spans over  $180^\circ$  centered on the downshear right (DSR) quadrant. The corresponding icosagon (Fig. 5i) shows that most flashes occur downshear in a much narrower region (span of  $\sim 60^\circ$ ), with

a slight downshear left (DSL) tendency. The icosagon has a radius almost equal to 1 in this direction and almost equal to zero in all other directions, indicating a relatively small number of flashes occurring in all other directions. To state it another way, there are plenty of flash occurrences spanning the  $180^\circ$  centered on the DSR direction, but in the ITPs where this happens, the vast majority of the flashes are actually located DSL of the center.

Figures 5h and 5i (for the evaluation domain) and Figs. 5k and 5l (for the open ocean) show that shear greater than  $5 \text{ m s}^{-1}$  induces a consistent DSL asymmetry. This asymmetry spans an azimuthal region that is reduced with the strength of the shear, as for moderate shear the region of maximum activity spans  $\sim 130^\circ$  (Figs. 5h,k), whereas for strong shear cases it is reduced by more than half, spanning only  $\sim 60^\circ$  (Figs. 5i,l). The asymmetry is centered on the DSL direction for moderate shear and is closer to directly downshear for strong shear. The fact that these

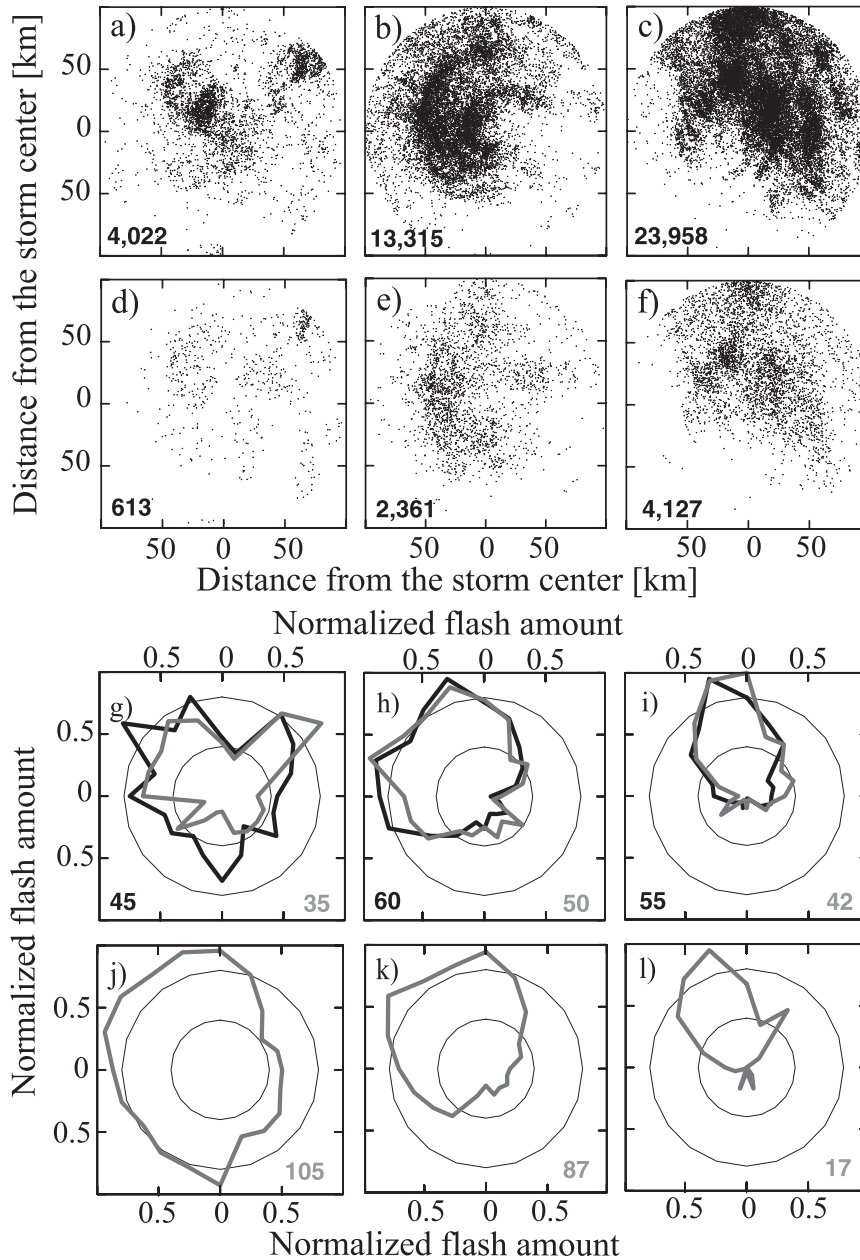


FIG. 5. (a)–(f) Inner core lightning locations and (g)–(l) icosagons for (left) weak ( $<5 \text{ m s}^{-1}$ ), (middle) moderate ( $5\text{--}10 \text{ m s}^{-1}$ ), and (right) strong ( $>10 \text{ m s}^{-1}$ ) shear. The shear vector is directed upward in each case. The evaluation domain is shown in the first three rows and the open ocean domain in the fourth. NLDN (WWLLN) locations are shown in the first (second) row. In the lower left corner of the panels, the number of flashes is presented. The third row shows the NLDN (WWLLN) icosagons and the number of ITPs available for each case in black (gray). The fourth row shows the WWLLN also with the number of ITPs available. The icosagon panels show two reference concentric circles at the 0.4 and 0.8 radii.

characteristics are observed in both domains suggests they are a robust feature of TCs under the influence of shear. The results of the present study are consistent with the findings of CM02, but the higher azimuthal resolution of this study suggests a narrowing of the region with the most

electrically active convection as the magnitude of the shear increases.

Although the downshear side of the storm is more electrically active in the weak shear cases (Figs. 5a,d), Figs. 5g and 5j show that weak shear does not induce

a clear asymmetry in lightning location. The shape of the icosagons in the evaluation domain (Fig. 5g) is not circular, but it lacks a defined azimuthal region of increased activity. With a larger number of ITPs, the open ocean domain (Fig. 5j) shows a more axisymmetric distribution of convective activity. Note that unlike the other cases, the discrepancy between the icosagons for the two networks is relatively large in the weak shear cases. This might be a result of both the small number of flashes in these cases (Figs. 5a,d) and the lack of an asymmetry in nature.

CM02 and CM03 provide a complete discussion on the physical interpretation of the asymmetries they found, which are confirmed here, including balanced flow arguments (Raymond 1992; Jones 1995; DeMaria 1996) and vortex interactions in the vertical (Jones 1995, 2000). More recently, Reasor et al. (2004) explained the inner core asymmetries of TCs in the presence of vertical shear based on vortex Rossby waves and their damping. However, none of these perspectives can account for the reduction of the azimuthal region of active convection with increased shear magnitude suggested by the results of this study.

### b. Shear asymmetries in the outer bands

Figure 6 is similar to Fig. 5, but for the outer rainband region, 100–300 km from the TC center. Similar to the inner core region, the lightning locations relative to the storm center (Figs. 6a–f) roughly show the preferred direction of electrical discharge activity. They can be compared to the icosagons to get a sense of the two representations of the asymmetries. As pointed out above, although flash locations can be illustrative, they can be misleading as well. Figure 6b shows an area of large activity DSL (in the inner part of the outer bands, ~100–150 km from the center). Despite the large number of flashes, the icosagon does not have a large value in that direction because the large number of flashes occurred in only one ITP that had an even larger number of DSR flashes.

Figures 6h, 6i, 6k, and 6l show that for moderate and strong shear magnitudes there is a preference for lightning to be located in the DSR quadrant. Figure 6g, showing the cases of weak shear in the evaluation domain, suggests a DSR asymmetry; however Fig. 6j, which shows cases of weak shear in the open ocean, shows only a downshear asymmetry, with no right or left preference. The difference between Figs. 6g and 6j might be related to the fact that stronger TCs (better represented in the open ocean domain as shown in Fig. 4) may be less affected by shear, exhibiting a more symmetric azimuthal distribution of convection. Overall, these results are in general agreement with CM02, who reported a DSR asymmetry for shear  $>5 \text{ m s}^{-1}$  in the outer bands, with no preference between DSL or DSR for the weakest shear category.

### c. Motion-induced asymmetries

Figure 7 shows the icosagons for slow, moderate, and fast motion categories obtained with the motion vector pointing north for both the evaluation and open ocean domains. It shows that the asymmetries associated with motion, again well captured by the WWLLN, are less clearly defined than those associated with shear. In the evaluation domain, a preference for the right front (RF) quadrant can be distinguished for the fast motion ITPs in both the inner core (Fig. 7c) and the outer bands (Fig. 7i). This asymmetry can also be distinguished in the inner core of the moderate motion cases (Fig. 7b) and to a lesser extent in the outer bands (Fig. 7h). In the open ocean domain, a preference for the right side of the storm can be distinguished for all of the moderate and fast motion cases, but with a preference for the right rear quadrant of the storms (Figs. 7e,f,k,l). As in the case of vertical wind shear, clear asymmetries are absent in the weaker magnitude cases (Figs. 7a,d,g,j).

Given the dominance of the vertical wind shear asymmetry as reported by CM03, Chen et al. (2006), and Ueno (2007), the asymmetries seen in the motion-rotated plots could be explained by the relationship between the motion and the shear vectors in the study domains. Figure 8a shows the angle between the shear and motion vectors for each ITP in the evaluation domain. These angles are found to hold the relationship described in CM03, with 51% of the ITPs having a motion vector between  $0^\circ$  and  $90^\circ$  left of (counterclockwise from) the shear vector, with a maximum between  $15^\circ$  and  $45^\circ$ . This relationship results from west or southwest shear, and motion with a northward component when TCs are near the U.S. shore (not shown). With this configuration, the motion-rotated lightning distributions in Fig. 7 would have a shear vector directed to the right, which would induce a DSL and RF asymmetry in the inner core (Figs. 7b,c) and a DSR and right, or rear right, asymmetry in the outer bands (Figs. 7h,i).

In the open ocean domain, the distribution of angles between the shear and motion vectors takes on a much broader shape (Fig. 8b). In this domain there are two shear regimes: a westerly regime (68% of the cases), as in the evaluation domain; and a less well-defined easterly regime (32% of the cases), for storms that are located farther south within the trade winds. In the westerly shear regime, where storms move to the west or west-northwest, the angles between the shear and motion vectors range from  $105^\circ$  to  $195^\circ$ . With this configuration, the panels referring to the open ocean domain in Fig. 7 would have a shear vector directed to the right or right rear of the motion vector, which would induce a right of motion asymmetry in the inner core (Figs. 7e,f) and rear asymmetry in the outer

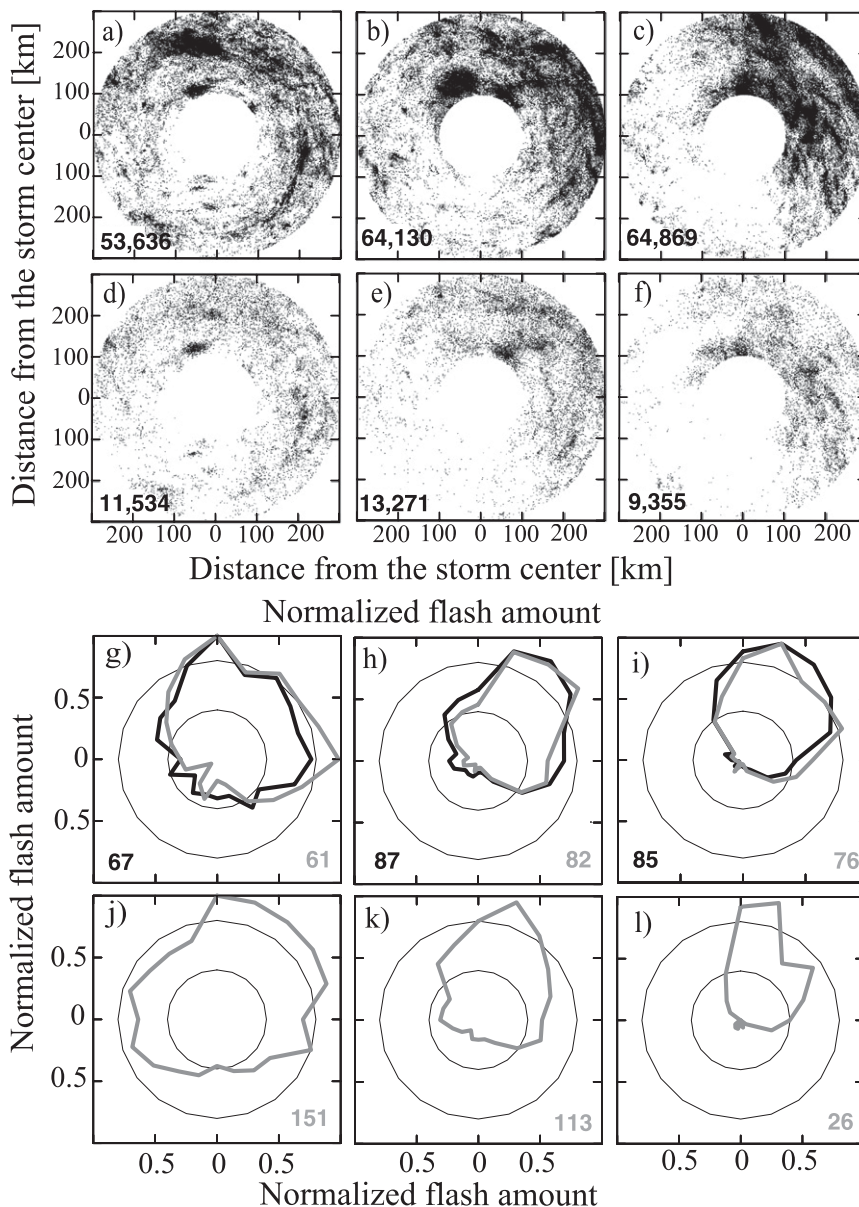


FIG. 6. As in Fig. 5, but for the outer band region.

bands (Figs. 7k,l). For the easterly regime, the angles between the motion and shear vectors take on a range of values centered around  $315^\circ$ . In this configuration, the panels referring to the open ocean domain in Fig. 7 would have a shear vector directed to the left of the motion vector, which would induce a left of motion asymmetry in the inner core and a front left motion asymmetry in the outer bands. Given that the easterly regime is less common than the westerly regime, its asymmetries are less clear in Fig. 7, but they can be weakly distinguished in both the inner core (Fig. 7e, and to a lesser extent Fig. 7f) and the outer bands (Fig. 7l).

### 7. Radial distribution of flash density

#### a. Total flash density as a function of radius

Figures 9a and 9b show the average radial flash density distributions in the evaluation domain (note that the average WWLLN profile was multiplied by 5 to facilitate easy network comparison). The plots show that when taking the average profile, the inner core appears to be the most electrically active region of the storm, being roughly 3 times more active than the rainbands. This figure is consistent with the results of the oceanic domain presented in Fig. 3 and agrees with the results of DeMaria

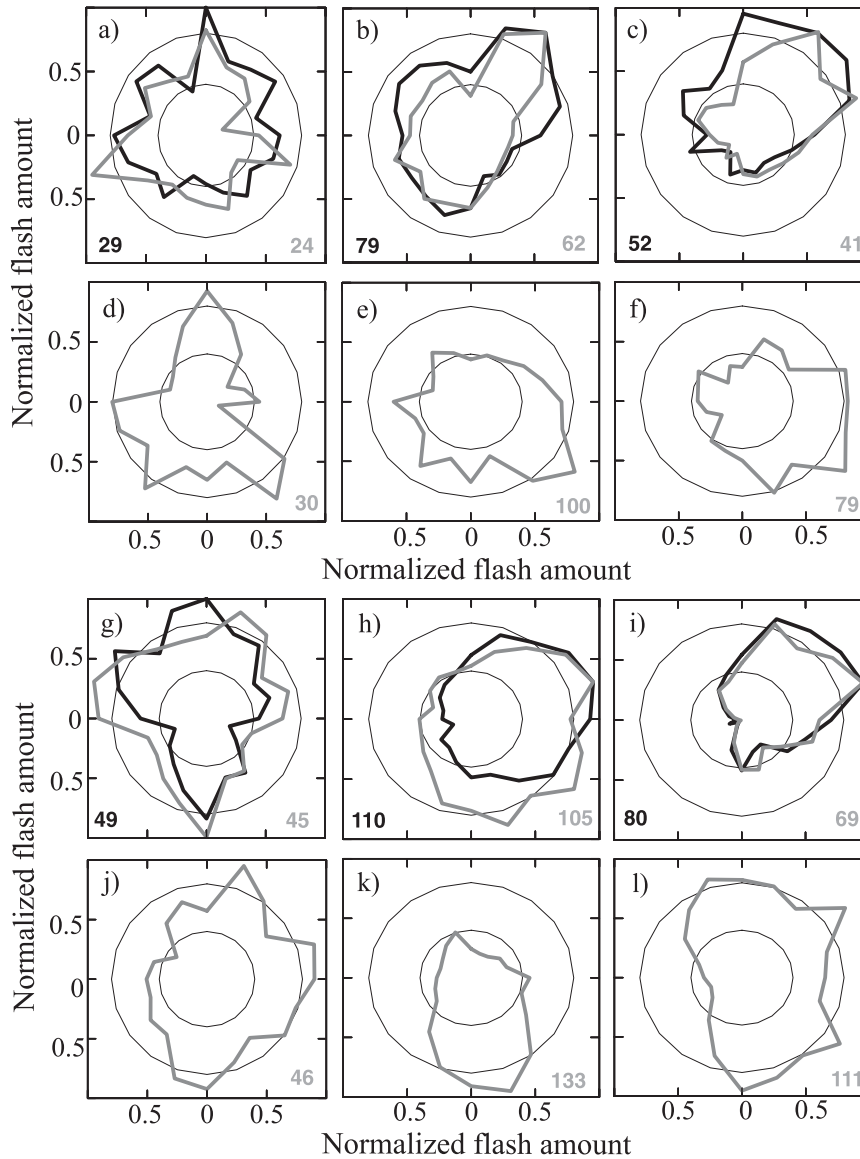


FIG. 7. (a)–(f) Inner core and (g)–(l) outer band icosagons for (left) slow ( $0\text{--}3\text{ m s}^{-1}$ ), (middle) moderate ( $3\text{--}6\text{ m s}^{-1}$ ), and (right) fast ( $>6\text{ m s}^{-1}$ ) motion. The evaluation (open ocean) domain is shown in the first and third (second and fourth) rows. NLDN (WWLLN) icosagons are shown in black (gray). The number of ITPs available for each case is shown in each panel. The motion vector is directed upward in each case. Also shown are two reference concentric circles at 0.4 and 0.8 radii.

and DeMaria (2009) and Yokoyama and Takayabu (2008), who suggested, following Cecil et al. (2002), that the lack of an outer core maximum could be due to a larger proportion of IC flashes in the inner core [not accounted for in Molinari et al. (1999) since they used NLDN data]. However, the tendency of the WWLLN (which measures some IC flashes) to underestimate flash density, as compared to the NLDN (which does not target IC flashes), in the inner core region of Fig. 9b suggests that a larger

proportion of IC flashes is not responsible for the difference in radial structure.

When describing the radial structure of flash density, however, the average may not be the most illustrative parameter, as the data distribution in each radial bin is highly skewed from 12 215 (1175) in the NLDN (WWLLN) down to 1 (both networks). Another, perhaps more meaningful, way to look at the flash density radial distribution is assigning equal weight to each ITP before

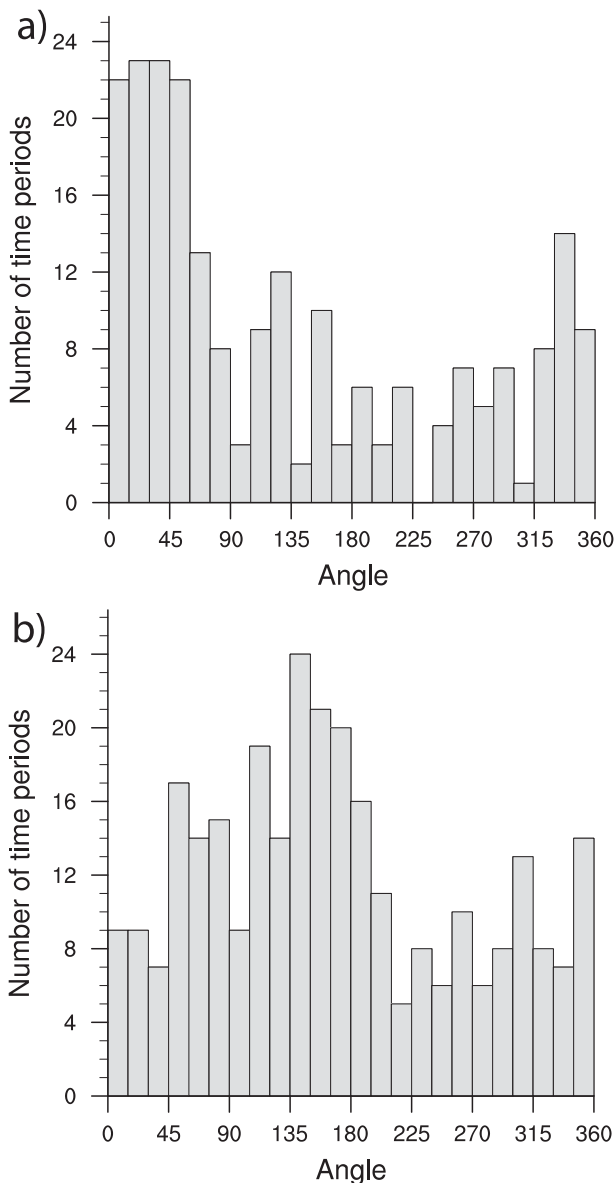


FIG. 8. Angle between the shear and motion vectors for each ITP measured counterclockwise from the vertical shear to the motion vector for (a) the evaluation domain and (b) the open ocean domain.

averaging. With this technique, each ITP is considered equally representative of the lightning activity regardless of the number of flashes, and the composite distribution is not obscured by a few ITPs with a large number of flashes (taking the median leads to similar results).

Figures 9c and 9d show the normalized average flash density of the equally weighted ITPs and illustrate that TCs tend to have three distinct regions of electrical activity: a relatively active region within the three bins closest to the center, a less active region centered around the 100-km radius, and a third region of increasing lightning activity

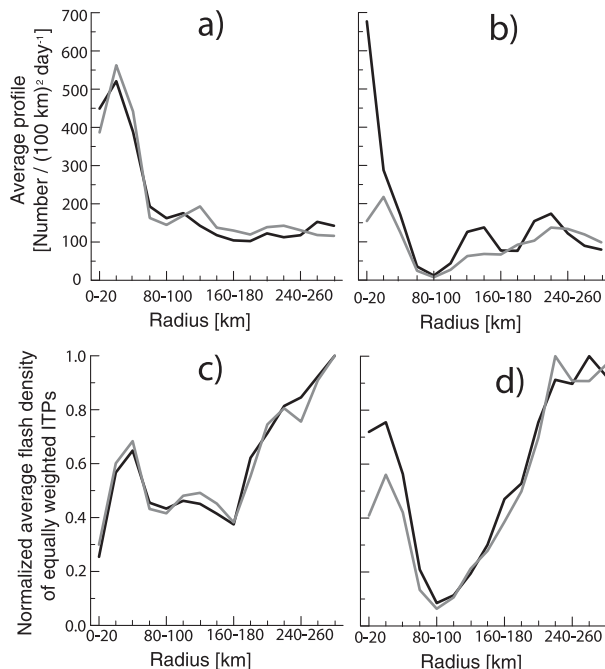


FIG. 9. Flash density radial structure in the evaluation domain. (a),(b) Average and (c),(d) composite, giving equal weight to each ITP. The left (right) column shows nonhurricane (hurricane) ITPs; the black (gray) lines show the NLDN (WLLN) curves. The average WLLN flash density was multiplied by a factor of 5 in the top row to facilitate comparison with the NLDN.

with radius. The last region contains the largest flash density in the radial range, both in hurricane and nonhurricane cases and is thought to be representative of the background non-TC environment (Bogner et al. 2000; Houze 2010). Although this general radial pattern is common between the two TC strength categories, there are differences between them as well. Hurricane ITPs tend to have a more accentuated distinction between the features with a more active core and a more pronounced region with weak activity. This second region is narrower in hurricane ITPs, extending between 60- and 120-km radii, and broader in the nonhurricane ITPs, going from 40- to 180-km radii.

While the three radial regions described are a clear feature of the composite, there is large interstorm variability with some hurricanes having a relatively more active inner core region and weaker electrical activity in the outer bands [e.g., Katrina (2005), Ophelia (2005), Rita (2005), and Wilma (2005)], while others show the opposite pattern [e.g., Ivan (2004), Jeanne (2004), and Cindy (2005)]. Only Tropical Storm Arlene (2005) showed comparable flash density in the inner core and the outer bands. There were also systems with the maximum of flash activity around the 100-km radius; however, all of these systems were relatively disorganized and none of them

reached hurricane strength [i.e., Hermine (2004), Matthew (2004), Tammy (2005), Alberto (2006), and Erin (2007)].

The hurricane composite results herein are consistent with the three radial regions first identified by Molinari et al. (1994, 1999), who called them the eyewall, inner band, and outer band, and with Cecil et al. (2002). Molinari et al. (1999) also described the radial evolution of three storms at nonhurricane stage that did not exhibit the described radial regions; however, their sample was small, consisting of only 144 h of data. With such a small sample, the episodic nature of lightning can obscure the results. The larger sample in this study, with a total of 1050 h of nonhurricane ITPs shows that prehurricane TCs also tend to have the structure of three radial regions, although they are less pronounced than their hurricane counterparts.

### b. Flash density by peak current

To further characterize the electrical activity of TCs as they become organized, an analysis of flash density by peak current was performed. Figure 10 shows the average NLDN negative<sup>1</sup> flash density for both hurricane and nonhurricane ITPs divided into bins of 30 kA. The overall (from 0 to 300 km) negative flash density is lower in hurricane strength ITPs than in nonhurricane ITPs and this difference is more pronounced as the flash peak current increases. For each of the bins considered, the flash density is smaller in hurricane ITPs, with the ratio decreasing from 0.70 in the weakest bin to 0.50 for the  $-90$  to  $-120$  kA bin. In the bin with the strongest flashes, the ratio increases again to 0.63. Given the episodic nature of lightning and the large variability in the number of flashes in a given storm, individual cases may not show a simple relationship between average TC intensity and flash frequency, but the results of Fig. 10 suggest that when compared with nonhurricane ITPs, hurricane ITPs tend to have fewer negative flashes and even fewer strong negative flashes.

With the diminution of flash density as the storms organize into hurricanes (Fig. 10), the radial distribution of flashes also changes. Figure 11 shows the radial distribution of NLDN negative flash density for different flash strengths. In the case of strong flashes, the flash density in nonhurricane ITPs is comparable in the inner core and in the outer bands, whereas for hurricane ITPs the flash density of strong flashes in the inner core is only  $\sim 0.5$  the value in the outer bands. In the case of weak flashes, the inner core/outer band ratio is comparable in hurricane ITPs and nonhurricane ITPs; that is, in

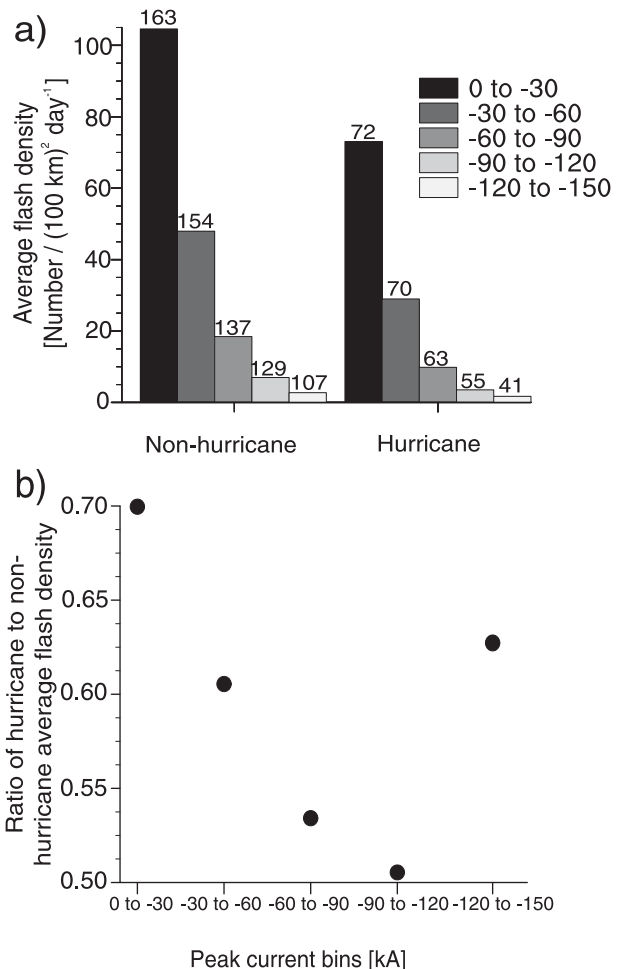


FIG. 10. (a) NLDN average negative flash density for hurricane and nonhurricane ITPs partitioned in bins of 30 kA; (b) the ratio of hurricane to nonhurricane average flash density. The number on top of each bar in (a) indicates the number of ITPs used for the average.

hurricane ITPs, which have fewer flashes than nonhurricane ITPs (Fig. 10), the reduction in flash occurrence is larger for stronger flashes than for weaker ones. Despite the close agreement between the networks in most of the bins of Figs. 9b and 9d, the WWLLN tends to underestimate the amount of flashes in the inner core of hurricanes. This underestimation might be the result of the large reduction of strong flashes in that region that results in a larger proportion of weaker flashes (Fig. 10), those most often missed by the WWLLN (Abarca et al. 2010).

The reduced amount of flashes in hurricane ITPs can be at least partially explained in the framework summarized by Black and Hallett (1999). In this view, more organized storms are more likely to have large amounts of ice from preexisting convection that could nucleate any incipient amount of supercooled water brought by updrafts above

<sup>1</sup> Positive flashes were not included because of the uncertainty in the weaker peak currents (see section 2) and the fast decrease of positive occurrences as peak current increases.

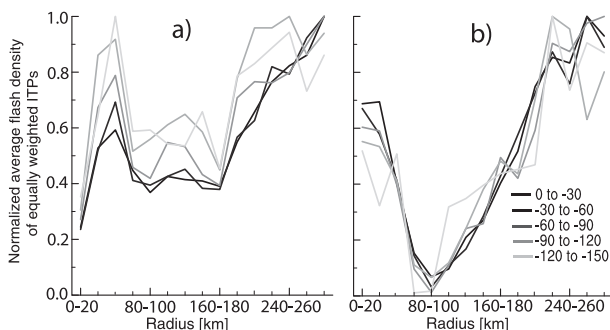


FIG. 11. NLDN normalized flash density of negative flashes separated by their maximum peak current (bins of 30 kA) for (a) nonhurricane and (b) hurricane ITPs. The shade of the lines is proportional to the magnitude of the current strength with 0 to  $-30$  kA corresponding to the darkest and  $-120$  to  $-150$  kA to the lightest shade.

the  $0^{\circ}\text{C}$  isotherm. In this scenario, more organized TCs are more likely to have a shallow mixed phase region and an ineffective charging of particles. However, inside the tropical cyclone aspects other than microphysics might be playing a role in determining the lightning occurrences. As shown in Figs. 9c and 9d, the reduction in the number of flashes occurs mostly in the inner band region, where it has been shown from observations (Houze 2010, his Fig. 32) that convection does not extend as high as in the inner band region. Houze (2010) suggested that the vertical confinement of the convection is probably the result of the strong radial outflow from the eyewall. Another aspect probably playing a role in the reduction of flash density in the inner core region of strong TCs is strain deformation induced by the vortex. Stronger vortices will induce stronger strain deformation that may result in filamentation times smaller than the convective overturning time scale, distorting or even suppressing convection as proposed by Rozoff et al. (2006).

While flash density modulation by microphysics and mesoscale dynamics can be explained, what determines the strength of flashes has not been explored as thoroughly. The results shown here suggest a strong relationship between flash strength and storm intensity, but detailed microphysics and mesoscale observations in conjunction with flash detection are necessary to elaborate hypotheses regarding the mechanisms involved.

## 8. Summary and conclusions

The lightning activity in 24 Atlantic basin tropical cyclones is investigated, focusing on flash density and storm asymmetries. Flash density is contrasted between intensifying and nonintensifying cases and is characterized as a function of TC intensity and radius. Our results suggest that flash density in the inner core is a parameter with

potential for distinguishing intensifying versus nonintensifying TCs. However, the largest potential lies in the weaker storm stages where flash density is the largest, and not in the stronger hurricane cases where most of the research in lightning and TC intensity has focused (e.g., Squires and Businger 2008; Price et al. 2009; Thomas et al. 2010).

The results of CM02 and CM03, regarding azimuthal asymmetries induced by vertical wind shear and storm motion, are confirmed here using the WWLLN for storms both close to the United States and over the open ocean and suggest that increasing vertical shear magnitude results in a narrowing of the azimuthal range of convective activity in the core. The three distinct regions of electrical activity originally proposed by Molinari et al. (1994) are also confirmed in our sample with a relatively active region close to the storm center, a less active region centered around the 100-km radius, and a third region of increasing lightning activity with radius for both hurricane and nonhurricane ITPs. A new result of this study is the strong relationship between flash peak current and storm intensity. Hurricane ITPs have fewer negative flashes than nonhurricane ITPs and the reduction in flash occurrence is larger for stronger flashes than for weaker ones.

Finally, the findings of this study suggest that despite the fact that the WWLLN locates only a small fraction of lightning occurrences, it can be successfully used to study mesoscale meteorological phenomena. The spatial correlation between TC lightning detected by the WWLLN and the NLDN is shown to be high. Also, both the azimuthal distribution of lightning and the radial structure of flash density were remarkably well captured by the WWLLN despite its low detection efficiency. The use of the WWLLN will be particularly useful in the study of TCs that form and evolve in the deep tropical oceans, away from the domain of any regional ground-based network.

*Acknowledgments.* The authors wish to thank the World Wide Lightning Location Network (<http://wwlln.net>), a collaboration among over 40 universities and institutions, for providing the lightning location data used in this paper. The National Lightning Detection Network data are provided through the Vaisala Thunderstorm Unit in Tucson, Arizona. The first author thanks Graciela B. Raga for her support at the beginning of this research. The manuscript was greatly improved by the careful suggestions of three anonymous reviewers.

## REFERENCES

- Abarca, S. F., K. L. Corbosiero, and T. J. Galarneau Jr., 2010: An evaluation of the Worldwide Lightning Location Network (WWLLN) using the National Lightning Detection Network

- (NLDN) as ground truth. *J. Geophys. Res.*, **115**, D18206, doi:10.1029/2009JD013411.
- Biagi, C. J., K. L. Cummins, K. E. Kehoe, and E. P. Krider, 2007: National Lightning Detection Network (NLDN) performance in southern Arizona, Texas, and Oklahoma in 2003–2004. *J. Geophys. Res.*, **112**, D05208, doi:10.1029/2006JD007341.
- Black, R. A., and J. Hallett, 1999: Electrification of the hurricane. *J. Atmos. Sci.*, **56**, 2004–2028.
- , H. B. Bluestein, and M. L. Black, 1994: Unusually strong vertical motions in a Caribbean hurricane. *Mon. Wea. Rev.*, **122**, 2722–2739.
- Boccippio, D. J., and Coauthors, 2000: The optical transient detector (OTD): Instrument characteristics and cross-sensor validation. *J. Atmos. Oceanic Technol.*, **17**, 441–458.
- Bogner, P. B., G. M. Barnes, and J. L. Franklin, 2000: Conditional instability and shear for six hurricanes over the Atlantic Ocean. *Wea. Forecasting*, **15**, 192–207.
- Cecil, D. J., and E. J. Zipser, 1999: Relationships between tropical cyclone intensity and satellite-based indicators of inner core convection: 85-GHz ice-scattering signature and lightning. *Mon. Wea. Rev.*, **127**, 103–123.
- , and —, 2002: Reflectivity, ice scattering, and lightning characteristics of hurricane eyewalls and rainbands. Part II: Intercomparison of observations. *Mon. Wea. Rev.*, **130**, 785–801.
- , —, and S. W. Nesbitt, 2002: Reflectivity, ice scattering, and lightning characteristics of hurricane eyewalls and rainbands. Part I: Quantitative description. *Mon. Wea. Rev.*, **130**, 769–784.
- Chen, S. S., J. A. Knaff, and F. D. Marks, 2006: Effects of vertical wind shear and storm motion on tropical cyclone rainfall asymmetries deduced from TRMM. *Mon. Wea. Rev.*, **134**, 3190–3208.
- Corbosiero, K. L., and J. Molinari, 2002: The effects of vertical wind shear on the distribution of convection in tropical cyclones. *Mon. Wea. Rev.*, **130**, 2110–2123.
- , and —, 2003: The relationship between storm motion, vertical wind shear and convective asymmetries in tropical cyclones. *J. Atmos. Sci.*, **60**, 366–376.
- Cramer, J. A., and K. L. Cummins, 1999: Long-range and transoceanic lightning detection. Preprints, *11th Int. Conf. on Atmospheric Electricity*, Guntersville, AL, Amer. Meteor. Soc., 250–253.
- Crombie, D. D., 1964: Periodic fading of VLF signals received over long paths during sunrise and sunset. *J. Res. Natl. Bur. Stand. (U.S.)*, **68D**, 27–34.
- Cummins, K. L., and M. J. Murphy, 2009: An overview of lightning locating systems: History, techniques, and data uses, with an in-depth look at the U.S. NLDN. *IEEE Trans. Electromagn. Compat.*, **51**, 499–518.
- , R. B. Pyle, and G. Fournier, 1999: An integrated North American lightning detection network. Preprints, *11th Int. Conf. on Atmospheric Electricity*, Guntersville, AL, Amer. Meteor. Soc., 218–221.
- DeMaria, M., 1996: The effect of vertical shear on tropical cyclone intensity change. *J. Atmos. Sci.*, **53**, 2076–2087.
- , and R. T. DeMaria, 2009: Applications of lightning observations to tropical cyclone intensity forecasting. Preprints, *16th Conf. on Satellite Meteorology and Oceanography*, Phoenix, AZ, Amer. Meteor. Soc., 1.3. [Available online at [http://ams.confex.com/ams/89annual/techprogram/paper\\_145745.htm](http://ams.confex.com/ams/89annual/techprogram/paper_145745.htm).]
- Demetriades, N. W., and R. L. Holle, 2005: Long-range lightning applications for hurricane intensity. Preprints, *First Conf. on Meteorological Applications of Lightning Data*, San Diego, CA, Amer. Meteor. Soc., P2.8. [Available online at [http://ams.confex.com/ams/Annual2005/techprogram/paper\\_84498.htm](http://ams.confex.com/ams/Annual2005/techprogram/paper_84498.htm).]
- , and —, 2006: Long-range lightning nowcasting applications for tropical cyclones. Preprints, *Second Conf. on Meteorological Applications of Lightning Data*, Atlanta, GA, Amer. Meteor. Soc., P2.15. [Available online at [http://ams.confex.com/ams/Annual2006/techprogram/paper\\_99183.htm](http://ams.confex.com/ams/Annual2006/techprogram/paper_99183.htm).]
- , M. J. Murphy, and J. A. Cramer, 2010: Validation of Vaisala's Global Lightning Dataset (GLD360) over the continental United States. Preprints, *29th Conf. on Hurricanes and Tropical Meteorology*, Tucson, AZ, Amer. Meteor. Soc., 16D.2. [Available online at [http://ams.confex.com/ams/29Hurricanes/techprogram/paper\\_168042.htm](http://ams.confex.com/ams/29Hurricanes/techprogram/paper_168042.htm).]
- Fleener, S. A., C. J. Biagi, K. L. Cummins, E. P. Krider, and X.-M. Shao, 2009: Characteristics of cloud-to-ground lightning in warm-season thunderstorms in the central Great Plains. *Atmos. Res.*, **91**, 333–352, doi:10.1016/j.atmosres.2008.08.011.
- Houze, R. A., Jr., 2010: Clouds in tropical cyclones. *Mon. Wea. Rev.*, **138**, 293–344.
- Jacobson, A. R., R. Holzworth, J. Harlin, R. Dowden, and E. Lay, 2006: Performance assessment of the World Wide Lightning Location Network (WWLLN), using the Los Alamos Sferic Array (LASA) array as ground truth. *J. Atmos. Oceanic Technol.*, **23**, 1082–1092.
- Jones, S. C., 1995: The evolution of vortices in vertical shear. I: Initially barotropic vortices. *Quart. J. Roy. Meteor. Soc.*, **121**, 821–851.
- , 2000: The evolution of vortices in vertical shear. III: Baroclinic vortices. *Quart. J. Roy. Meteor. Soc.*, **126**, 3161–3185.
- Kummerow, C., W. Barnes, T. Kozu, J. Shiue, and J. Simpson, 1998: The Tropical Rainfall Measuring Mission (TRMM) sensor package. *J. Atmos. Oceanic Technol.*, **15**, 809–817.
- Lay, E. H., R. H. Holzworth, C. J. Rodger, J. N. Thomas, O. Pinto, and R. L. Dowden, 2004: WWLL global lightning detection system: Regional validation study in Brazil. *Geophys. Res. Lett.*, **31**, L03102, doi:10.1029/2003GL018882.
- Leary, L. A., and E. A. Ritchie, 2009: Lightning flash rates as an indicator of tropical cyclone genesis in the eastern North Pacific. *Mon. Wea. Rev.*, **137**, 3456–3470.
- Molinari, J., and D. Vollaro, 1989: External influences on hurricane intensity. Part I: Outflow layer eddy angular momentum fluxes. *J. Atmos. Sci.*, **46**, 1093–1105.
- , P. K. Moore, V. P. Idone, R. W. Henderson, and A. B. Saljoughy, 1994: Cloud-to-ground lightning in Hurricane Andrew. *J. Geophys. Res.*, **99**, 16 665–16 676.
- , P. Moore, and V. Idone, 1999: Convective structure of hurricanes as revealed by lightning locations. *Mon. Wea. Rev.*, **127**, 520–534.
- Pessi, A. T., S. Businger, K. L. Cummins, N. W. Demetriades, M. Murphy, and B. Pifer, 2009: Development of a long-range lightning detection network for the Pacific: Construction, calibration, and performance. *J. Atmos. Oceanic Technol.*, **26**, 145–166.
- Pinto, I. R. C. A., and O. Pinto Jr., 2003: Cloud-to-ground lightning distribution in Brazil. *J. Atmos. Sol.-Terr. Phys.*, **65**, 733–737.
- Price, C., M. Asfur, and Y. Yair, 2009: Maximum hurricane intensity preceded by increase in lightning frequency. *Nat. Geosci.*, **2**, 329–332; Corrigendum, **2**, 244.
- Rakov, V. A., and M. A. Uman, 2003: *Lightning: Physics and Effects*. Cambridge University Press, 687 pp.
- Raymond, D. J., 1992: Nonlinear balance and potential-vorticity thinking at large Rossby number. *Quart. J. Roy. Meteor. Soc.*, **118**, 987–1015.

- Reasor, P. D., M. T. Montgomery, and L. D. Grasso, 2004: A new look at the problem of tropical cyclones in vertical shear flow: Vortex resiliency. *J. Atmos. Sci.*, **61**, 3–22.
- Rodger, C. J., J. B. Brundell, and R. L. Dowden, 2005: Location accuracy of VLF World-Wide Lightning Location (WWLL) network: Post-algorithm upgrade. *Ann. Geophys.*, **23**, 277–290.
- , S. Werner, J. B. Brundell, E. H. Lay, N. R. Thomson, R. H. Holzworth, and R. L. Dowden, 2006: Detection efficiency of the VLF World-Wide Lightning Location Network (WWLLN): Initial case study. *Ann. Geophys.*, **24**, 3197–3214.
- , J. B. Brundell, R. H. Holzworth, and E. H. Lay, 2009: Growing detection efficiency of the World Wide Lightning Location Network. *AIP Conf. Proc.*, **1118**, 15–20, doi:10.1063/1.3137706.
- Rozoff, C. M., W. H. Schubert, B. D. McNoldy, and J. P. Kossin, 2006: Rapid filamentation zones in intense tropical cyclones. *J. Atmos. Sci.*, **63**, 325–340.
- Samsury, C. E., and R. E. Orville, 1994: Cloud-to-ground lightning in tropical cyclones: A study of Hurricanes Hugo (1989) and Jerry (1989). *Mon. Wea. Rev.*, **122**, 1887–1896.
- Shao, X.-M., and Coauthors, 2005: Katrina and Rita were lit up with lightning. *Eos, Trans. Amer. Geophys. Union*, **86**, doi:10.1029/2005EO420004.
- Squires, K., and S. Businger, 2008: The morphology of eyewall lightning outbreaks in two category 5 hurricanes. *Mon. Wea. Rev.*, **136**, 1706–1726.
- Thomas, J. N., N. N. Solorzano, S. A. Cummer, and R. H. Holzworth, 2010: Polarity and energetics of inner core lightning in three intense North Atlantic hurricanes. *J. Geophys. Res.*, **115**, A00E15, doi:10.1029/2009JA014777.
- Ueno, M., 2007: Observational analysis and numerical evaluation of the effects of vertical wind shear on the rainfall asymmetry in the typhoon inner-core region. *J. Meteor. Soc. Japan*, **85**, 115–136.
- Yokoyama, C., and Y. N. Takayabu, 2008: A statistical study on rain characteristics of tropical cyclones using TRMM satellite data. *Mon. Wea. Rev.*, **136**, 3848–3862.